

DYNAMIC LOAD SHARING BETWEEN PARALLEL DC-DC CONVERTERS USING AN ANFIS CONTROLLER

**Rondi Babu¹, Sunke Rohini², Beerla Manideep³, Nalumachu Akshay Kumar⁴, Burra
Durga Nivas⁵**

¹Assistant Professor, Department of EEE, Jyothishmathi Institute of Technology and Science,
Nustulapur, Karimnagar, T.S., India

^{2,3,4,5}UG Students, Department of EEE, Jyothishmathi Institute of Technology and Science,
Nustulapur, Karimnagar, T.S., India

baburondi@gmail.com, rohinisunke@gmail.com, beerlamanideep@gmail.com,
akshaynalumachu@gmail.com, durganivasb@gmail.com

Abstract: Using an ANFIS controller, the primary objective of this project is to provide a DC micro grid with dynamic load sharing across DC-DC converters. The term "micro grid" refers to a smaller-scale power grid that may either function autonomously or in tandem with the larger electric grid. A control method using dc-dc converters is crucial for the effective functioning of micro grids. You may use any kind of direct current (dc) source, including solar cells, fuel cells, etc., as an input to a dc-dc converter. A major issue is the distribution of load among the converters. Systems that rely on communication and systems that rely on droop characteristics are the two main categories of load-sharing algorithms (without communication). This research takes a look at two dc-dc converters linked in parallel for the purpose of load sharing using the droop approach. There is a severe voltage imbalance on the dc bus when the loads are varied due to the drooping characteristics of the converters. We addressed this complexity by maintaining a constant voltage on the dc bus through regulating the voltage axis intercept of the droop characteristics. This approach also applies to the micro grid

output, which necessitates an ANFIS control system for grid synchronization with the main grid. We demonstrated these results using MALAB/SIMULINK.

Keywords: Micro grids, Adjustable Neuro-Fuzzy Inference Systems (ANFIS), and Dynamic Load Sharing are some of the terms used in this context.

I. INTRODUCTION

Distributed energy resources and loads that may function either in tandem with or apart from the larger power grid make up what is known as a micro grid. To power the DC bus loads, DC micro grids use a network of linked generators that run in parallel. According to [3], DC-DC converters link solar power plants and battery storage devices to the DC bus. A control system included in the DC-DC converters is necessary to allow load sharing between them, similar to the frequency droop characteristics of linked synchronous generators. Direct current (DC) generators may benefit from a voltage droop characteristic, which is similar to the frequency droop characteristics employed in AC (alternating current) generators [4]. An integrated control system that regulates the

voltage axis intercept of droop characteristics keeps the micro grid's DC bus voltage constant is implemented to handle this issue. This action raises the voltage droop line, which moves the operating point closer to the target DC bus voltage. This study showcases the load sharing management for a 48V DC bus and details the modelling and simulation of voltage droop characteristics and the ANFIS controller as they pertain to DC-DC buck converters. Also covered are the causes that ultimately resulted in the invention of the DC-DC buck converter.

II: Managing Load Sharing

(A) Features of Voltage Droop

A feature of direct current (DC) sources known as voltage droop is a clear decline in output voltage accompanied by a clear rise in the power output. Two sources' droop characteristics are schematically shown in Fig.1, and they may be mathematically generalized as,

$$V_1 = -m_1 P_1 + V_{NL} \quad (1)$$

$$V_2 = -m_2 P_2 + V_{NL} \quad (2)$$

in where m_1 and m_2 are the inclinations of the two sources' sagging lines. No load voltage (V_{NL}) is the voltage at which the sources begin to droop, as seen by the voltage axis intercept. The two sources' terminal voltages, V_1 and V_2 ,

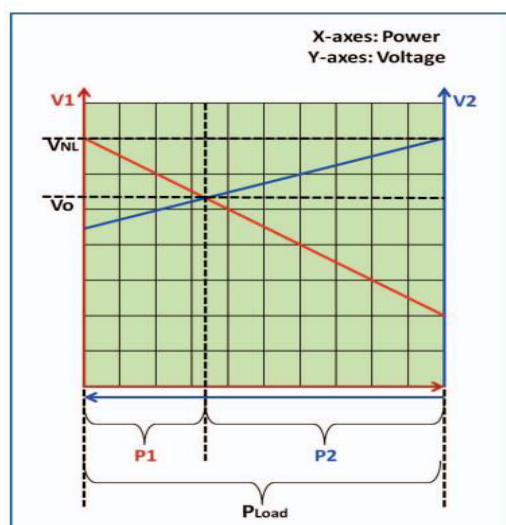


Fig. 1: Droop Characteristics of two DC sources/ DC-DC converters. V_0 is the operating point voltage of load resulted from intersection of droop characteristics.

P_1 and P_2 is the load shared by two sources out of total system load of P_{Load}

B) Load Sharing

$$P_1 + P_2 = P_{LOAD} \quad (3)$$

$$V_1 = V_2 \quad (4)$$

From equation eqn. 1, eqn. 2 and eqn. 4,

$$-m_1 P_1 + V_{NL} = -m_2 P_2 + V_{NL} \quad (5)$$

Equation eqn. 3 and eqn. 4 is a set of two simultaneous equations solution to which is stated as follows:

$$P_1 = P_{LOAD} * \frac{m_2}{(m_1 + m_2)} \quad (6)$$

$$P_2 = P_{LOAD} * \frac{m_1}{(m_1 + m_2)} \quad (7)$$

From eqn. 6 and eqn. 7,

$$\frac{P_1}{P_2} = \frac{m_2}{m_1} \quad (8)$$

C) Effect of internal resistance

$$V_1 = -m_1 P_2 + V_{NL} - I_1 R_1 \quad (9)$$

$$V_2 = -m_2 P_2 + V_{NL} - I_2 R_2 \quad (10)$$

When the DC sources' internal resistances are denoted by R_1 and R_2 , and the load currents provided by the DC sources are denoted as I_1 and I_2 , respectively. When the internal resistance of sources causes a change in the effective slope of droop characteristics, the load sharing across sources likewise changes according to these new effective slopes. It is simple to correct for the change in load sharing caused by internal resistances by adjusting the slopes of the characteristics.

III. CONSTANT VOLTAGE CONTROL (VOLTAGE AXIS INTERCEPT CONTROL)

The overall load on the system also determines the operating point voltage for the voltage droop characteristics [5]. The DC bus operating point voltage drops as the system load rises. To address this issue, the droop characteristics' voltage axis intercept (VNL) is adjusted. Doing so restores the operating point voltage to its appropriate value and elevates the droop characteristics. Figure 2 The load sharing for the slopes is still maintained, thus this doesn't alter anything. controlled voltage systems that remain constant. Load sharing is shown schematically in Fig. 3. A PID controller regulates the voltage axis intercept in a constant voltage control

system, which utilizes DC bus voltage as feedback. [2]

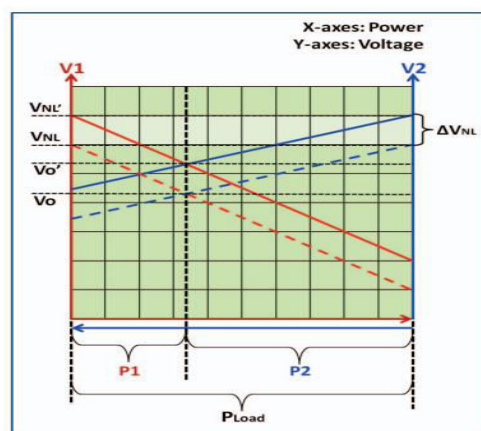


Fig. 2: Concept of constant voltage control: voltage axis intercept (V_{NL}) is varied to lift up the droop characteristics to increase the DC Bus operating voltage (from V_o to V_o') without varying the previous load sharing. ΔV_{NL} is the shift in the voltage axis intercepts.

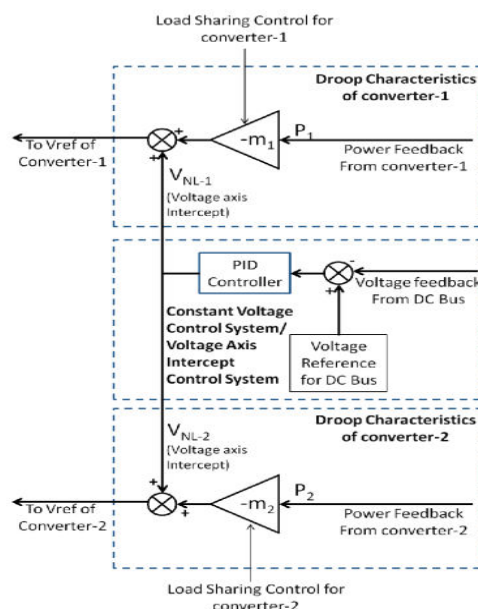


Fig. 3: Droop characteristics of sources and constant voltage control system controlling the voltage axis intercept.

IV. 48 VOLT DC BUS

In order to govern the load sharing of two DC-DC buck converters, this section details the design of a 48V constant DC bus based on the voltage droop characteristic.

The design of the Buck converter

The system's voltage is stepped down to 48 V DC bus rating by use of a buck converter. A single-phase buck converter designed in MATLAB is seen in Figure 4. To eliminate ripples in the output, it has a Misfit, an inductor, a diode, and a capacitor.

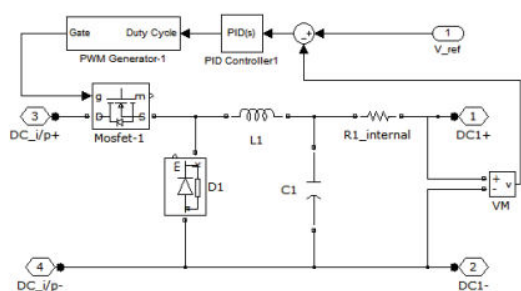


Fig. 4: DC-DC converter (as simulated in MATLAB Simulink)

A constant fixed frequency mode is used to run the converter. By selecting the optimal switching frequency, the converter is designed to maximize efficiency and minimize size [6]. In order to regulate the Misfit gate, a PID controller is used [2]. The inductor and output filter capacitor values are the most important factors in the functioning of a DC-DC converter. To decrease current ripple content in the output and ensure continuous operation even with tiny load current, the inductor value is computed. The output capacitor's job is to provide a constant voltage by absorbing ripple in the inductor's current. Before the regulator can respond, it must

also guarantee that the output can handle load stages. The values of the inductor and capacitor may be determined using the following formulae. [1]

$$L_{\text{mean}} = \frac{((V_{\text{in}(\text{min})} - V_{\text{out}}) * D_{\text{max}})}{(\Delta I_L * f)} \quad (11)$$

$$C_{\text{mean}} = \frac{1}{(8 * f * \frac{\Delta V_{\text{out}}}{\Delta I_L} - R_C)} \quad (12)$$

where, $V_{\text{in}(\text{min})}$ =minimum input voltage

V_{out} =output voltage

ΔI_L =inductor ripple current

D_{max} =maximum duty cycle

R_C =Equivalent series resistance of capacitor

B) PROPOSED ANFIS CONTROLLER

A sort of artificial neural network that is based on the Takagi-Surgeon fuzzy inference system is an Adaptive Neuro-Fuzzy Inference system (ANFIS). This method first emerged in the early '90s. It combines the best features of neural networks and fuzzy logic into one system, which might be quite useful. The inference mechanism is based on a collection of learnable fuzzy IF-THEN rules that can approximate nonlinear functions. This means that ANFIS may be used for any kind of estimate. Using the best settings determined by a genetic algorithm will help you operate the ANFIS more efficiently and optimally. An intelligent energy management system that is aware of its surroundings may make use of it. Figure 5 depicts a state-of-the-art ANFIS design.

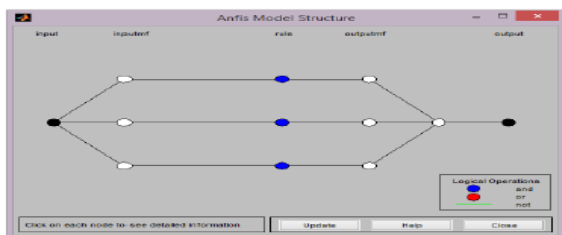


Fig.5 Optimized ANFIS architecture

In Fig.6 shows the proposed ANFIS based control architecture. The node functions of each layer in ANFIS architecture are described as follows:

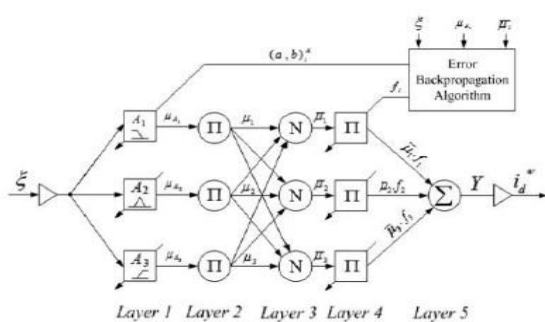


Fig.6 Schematic of the proposed ANFIS

The neuro-fuzzy controller is fed the difference between the reference and correct dc-link voltages, which is calculated as $\xi = V_{ac}^* - V_{ac}$. It uses this mistake, along with a similar one, to adjust the precondition and subsequent settings. The active power current segment (i_d^*) is obtained by controlling the dc-link voltage; it is further modified to measure the active current component injected from RES (I_{ren}).

Primary Level: Russification is applied to this layer. In this layer, we compute the degrees of the membership functions for all the input variables. For ANFIS, the error (e) and the change of error (Δe) are selected as the input variables. Figure 7 shows the use of trapezoidal and triangular enrolment capabilities to reduce

computation error. The following are the related node conditions:

$$O_i^1 = \mu_{Ai}(x) = \frac{1}{1 + \left[\frac{(x - c_i)}{a_i} \right]^{2b_i}} \quad (13)$$

Where x is the input to node I , A_i is the linguistic variable associated with this node function μ_{Ai} is the membership function of A_i , and $\{a_i, b_i, c_i\}$ is the premise parameter set.

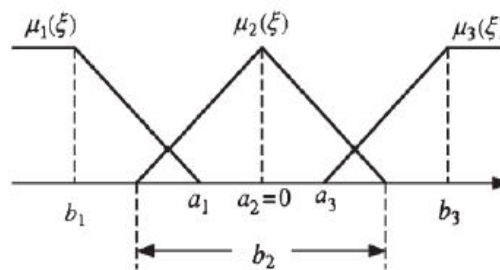


Fig. 7 Fuzzy membership functions.

Layer 2: This layer is rule inference layer. Every node in this layer is a fixed node labelled as Π which multiplies the incoming signals and sends the product out. Each node output corresponds to the firing strength of a fuzzy rule.

$$O_i^2 = \mu_i = \mu(x)\mu(y) \quad i = 1,2,3 \quad (14)$$

Layer 3: This layer is normalization layer. Every node in this layer is a circle node labelled N . The node calculates the ratio of the rule's firing strength to the sum of all rules' firing strength.

$$O_i^3 = \bar{\mu}_i = \frac{\mu_i}{\mu_1 + \mu_2 + \mu_3} \quad i = 1,2,3 \quad (15)$$

Layer 4: This layer is consequent layer. All nodes are an adaptive mode with node function

$$O_i^4 = \bar{\mu}_i \cdot f_i = \bar{\mu}_i (a_0^i + a_1^i \epsilon) \quad i = 1,2,3 \quad (16)$$

where win is the output of Layer 3 and (a₀, a₁) is the consequent parameter set.

Layer 5: This layer is output layer. The single node in this layer is a fixed node labelled Σ that computes the overall output as the summation of all incoming signals

$$O_i^5 = \mu_i = \sum_i \bar{\mu}_i f_i \quad i = 1,2,3 \quad (17)$$

The parameters of ANFIS are updated using the back propagation error term as follow:

$$\frac{\partial E}{\partial O^5} = k_1 \cdot e + k_2 \cdot \Delta e \quad (18)$$

The input signals error (e) and the change of error (Δe) multiplied by the coefficients k1 and k2.

$$\alpha_{k+1} = \alpha_k - \eta \frac{\partial E}{\partial \alpha_k} \quad (19)$$

where α is any of the parameters of ANFIS and η is learning rate. The error will be reduced next training iteration

V.SIMULATION RESULTS

1) EXISTING RESULTS

A. Load sharing without voltage axis intercept control

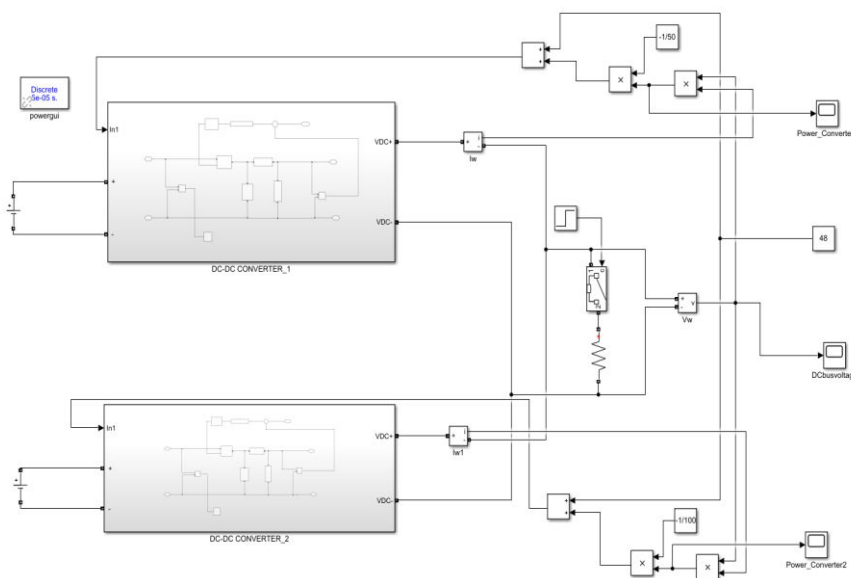


Fig. 8: Voltage droop characteristics for load sharing and without voltage control system (as simulated in MATLAB Simulink)

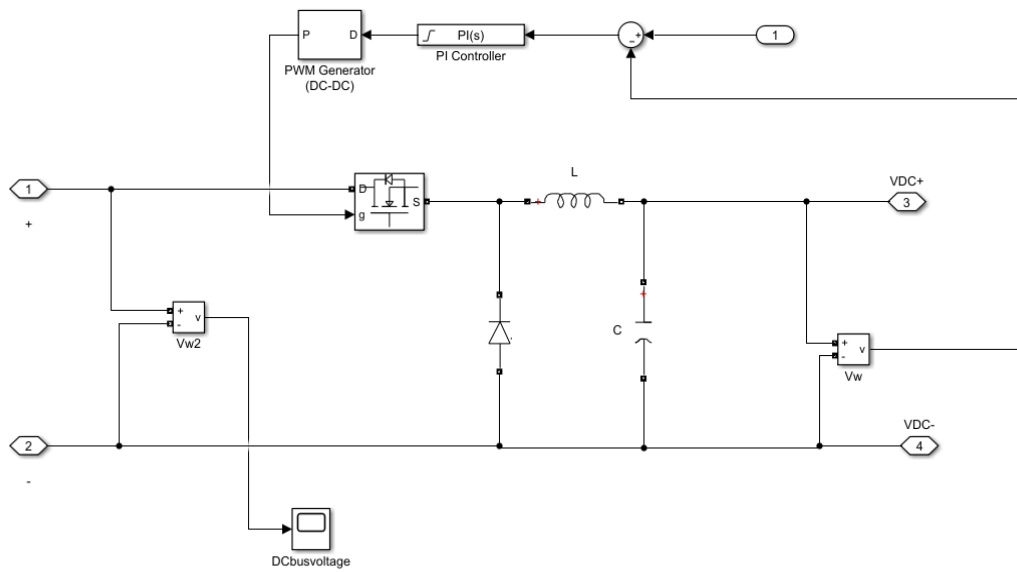
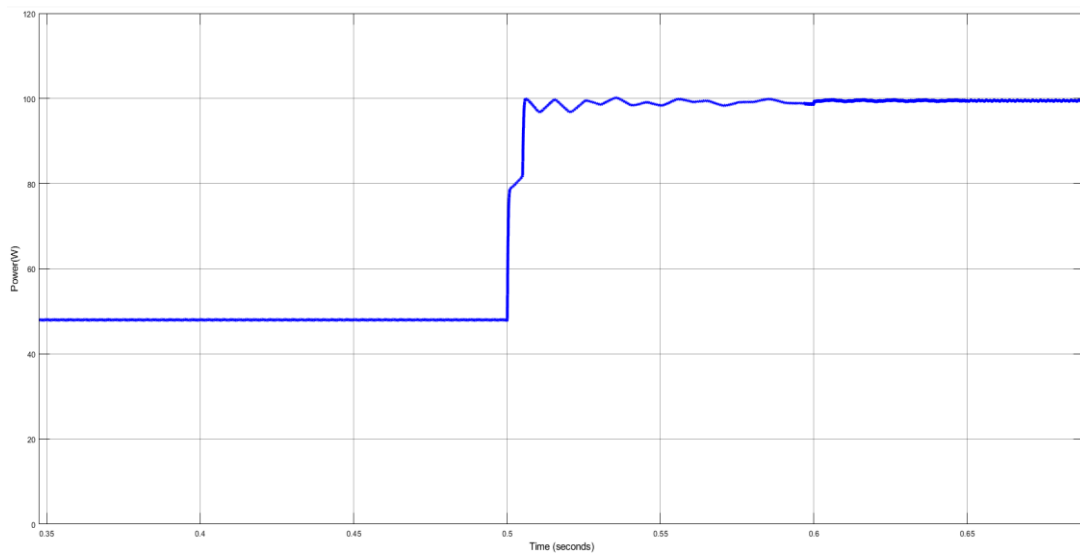


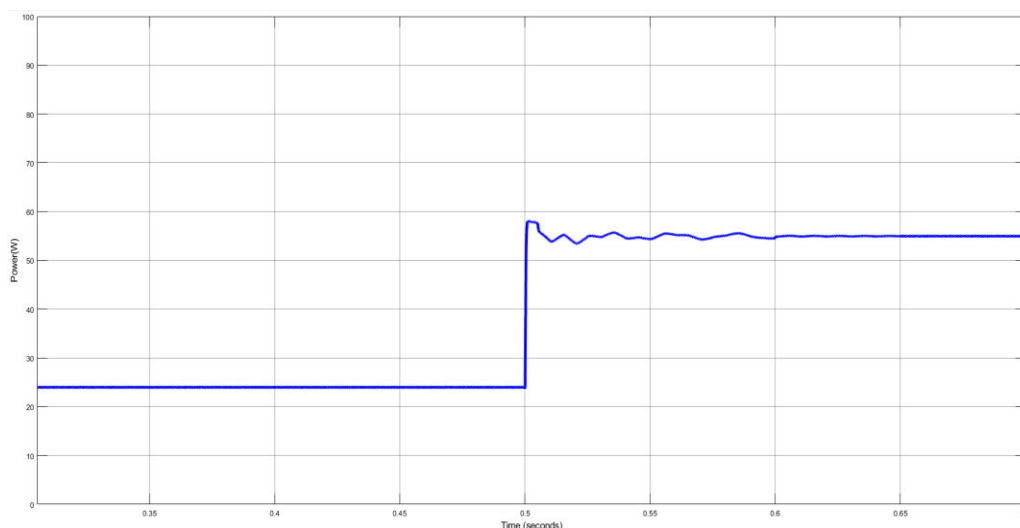
Fig.9 Buck converter circuit

At approximately 0.5 seconds, a sudden increase in load occurs, causing a disturbance in the system. The first subplot shows that Converter-1 responds to this change by increasing its output power to about 40W, with minor transient oscillations before settling.



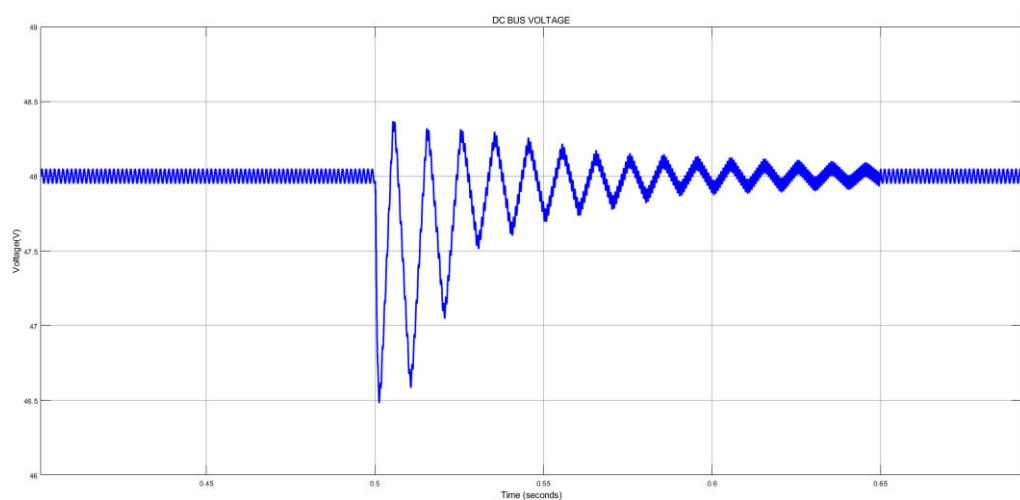
(a) Power of converter-1

The second subplot depicts Converter-2, which also reacts to the load disturbance. Its output power increases to around 80W, again with small oscillations that stabilize over time. This confirms that the 1:2 power sharing ratio between Converter-1 and Converter-2 is maintained even after the load change.



(b) Power of converter-2

The third subplot illustrates the DC bus voltage, which initially remains stable at 48V but then undergoes a sharp dip right after the load change, with oscillations that gradually dampen. Eventually, the voltage settles at a new steady-state value of 47.5V, indicating a 0.5V drop in the DC bus voltage due to the absence of voltage regulation.



(c) DC bus Voltage

Fig 10: Load sharing between converters and DC bus voltage WITHOUT constant voltage control system.

B. Load sharing with voltage axis intercept control

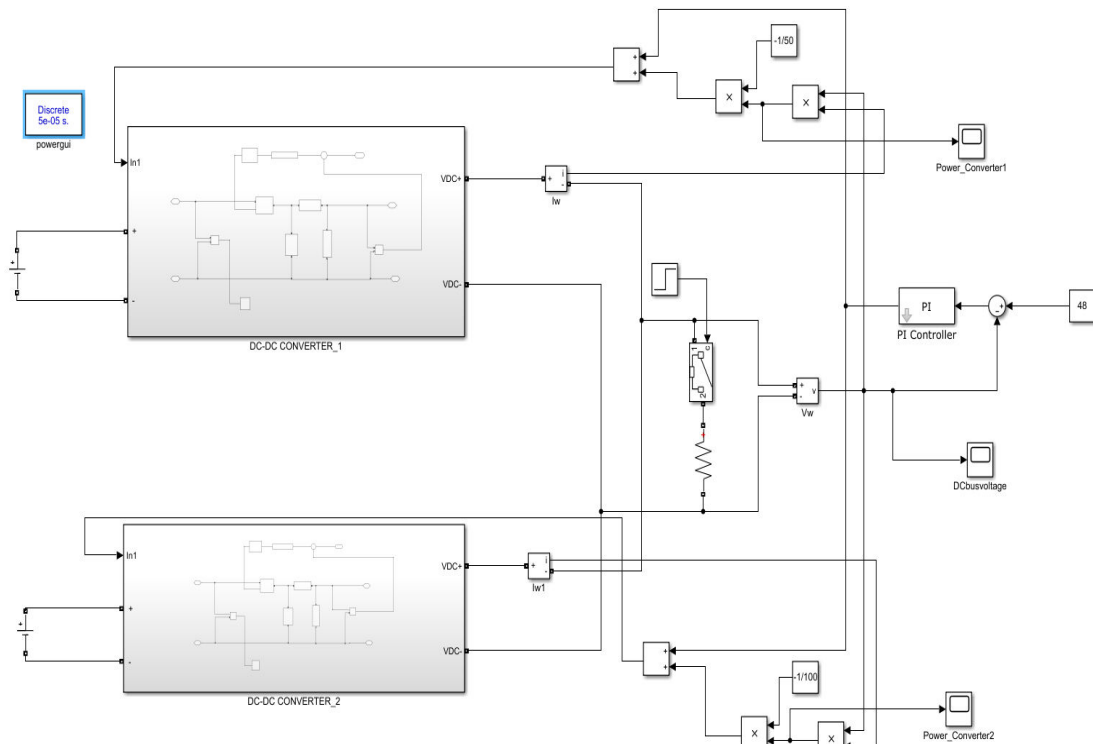
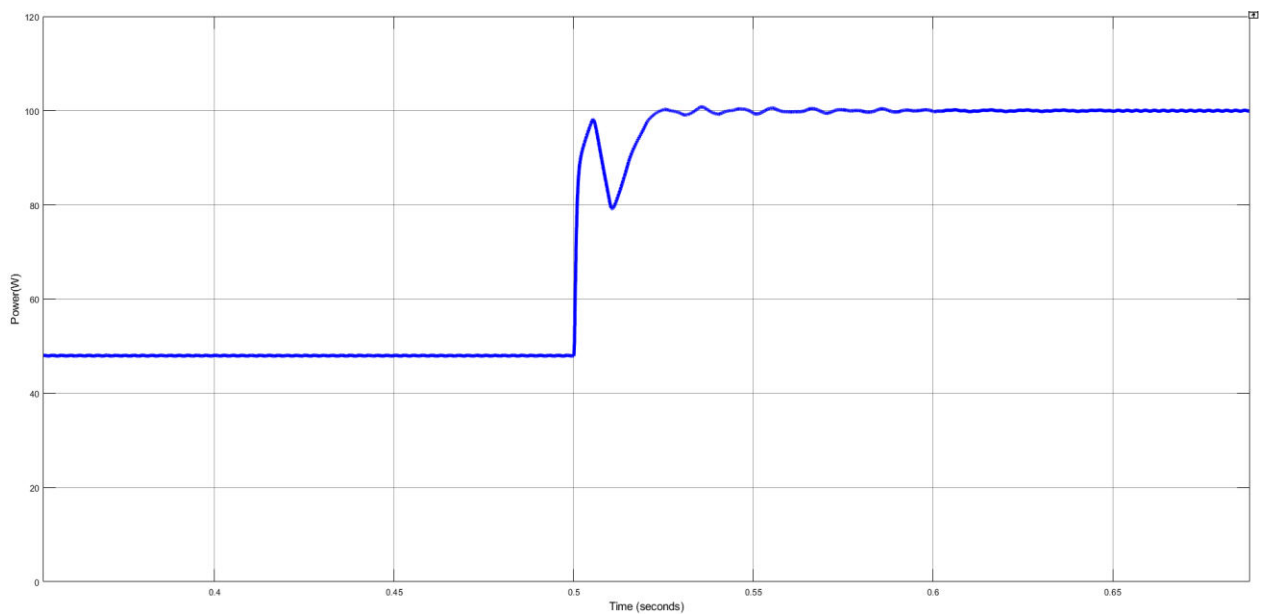


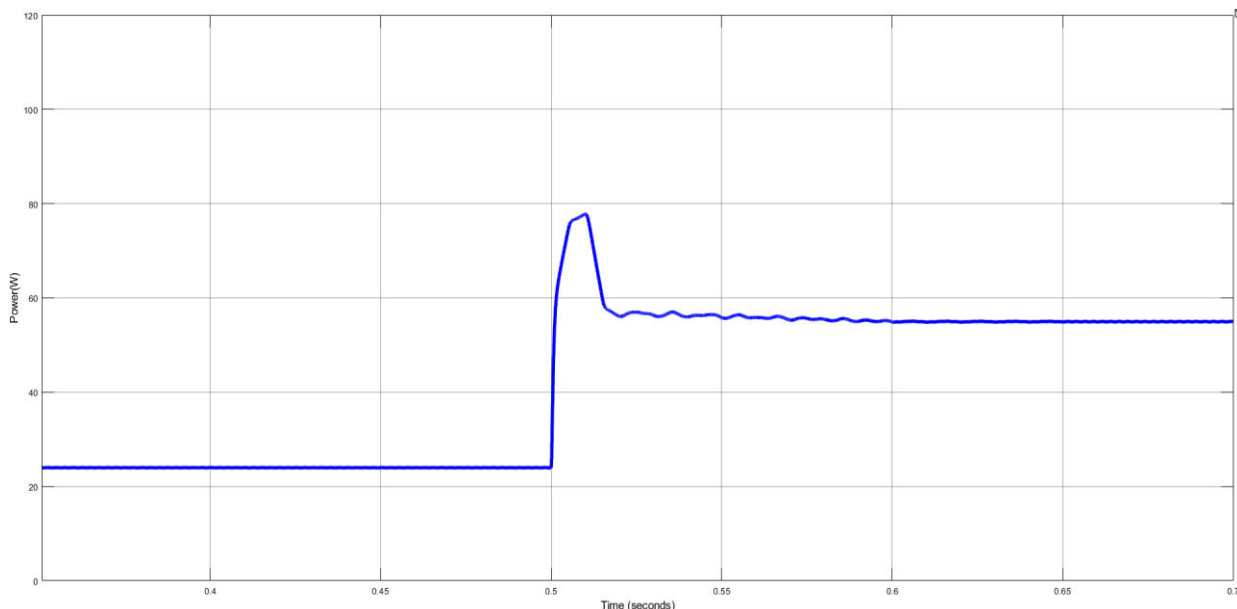
Fig 11: Voltage droop characteristics for load sharing and voltage control system (as simulated in MATLAB Simulink)

The first plot shows how Converter-1 responds to a sudden increase in load at around 0.5 seconds. Initially at zero, the power rapidly rises and stabilizes around 40 watts, with some minor oscillations during the transient phase. This indicates that Converter-1 quickly adjusts to the new load condition, contributing one part of the total power.



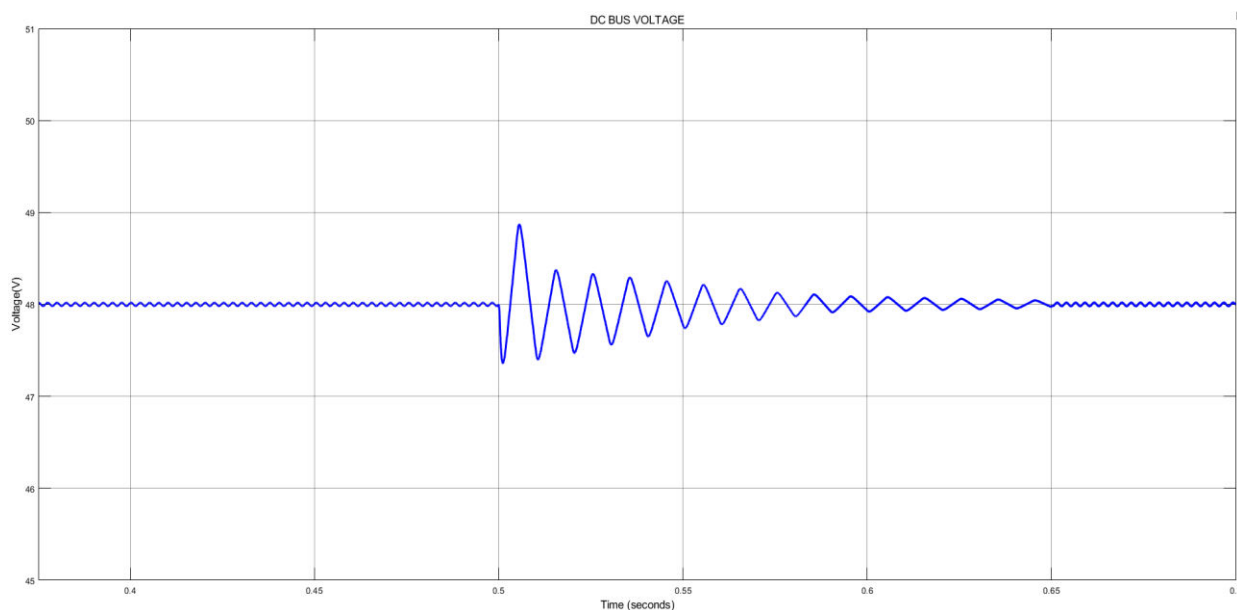
(a) Power of converter-1

In the second plot, Converter-2 displays a similar dynamic response. The power jumps from zero to approximately 80 watts, also showing a brief oscillatory behaviour before settling. This higher power level compared to Converter-1 confirms that it continues to supply twice the power, maintaining the 1:2 sharing ratio.



(b) Power of converter-2

The below plot captures the DC bus voltage profile. Following the load disturbance at 0.5 seconds, the voltage momentarily drops and exhibits damped oscillations. Thanks to the voltage control using a PID controller, these oscillations are progressively reduced, and the voltage returns to the nominal value of 48 volts. This reflects successful regulation despite dynamic changes in the system.



(c) DC bus Voltage

Fig 12: Load Sharing between two converters and DC bus voltage with constant voltage control/ voltage axis intercept control activate

2) EXTENSION RESULTS

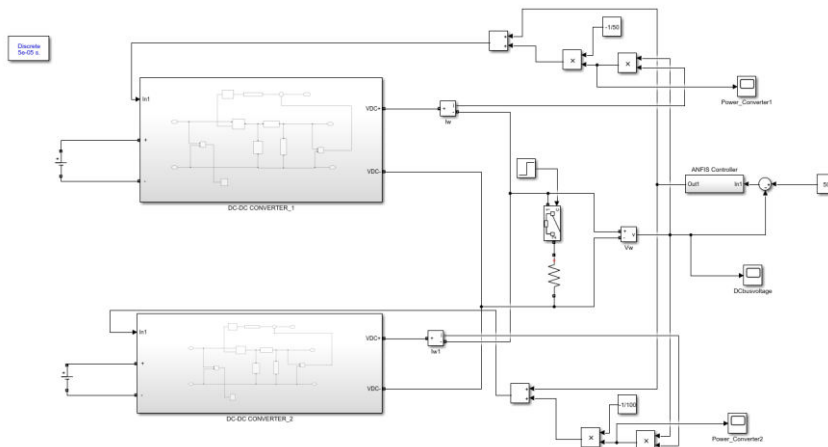
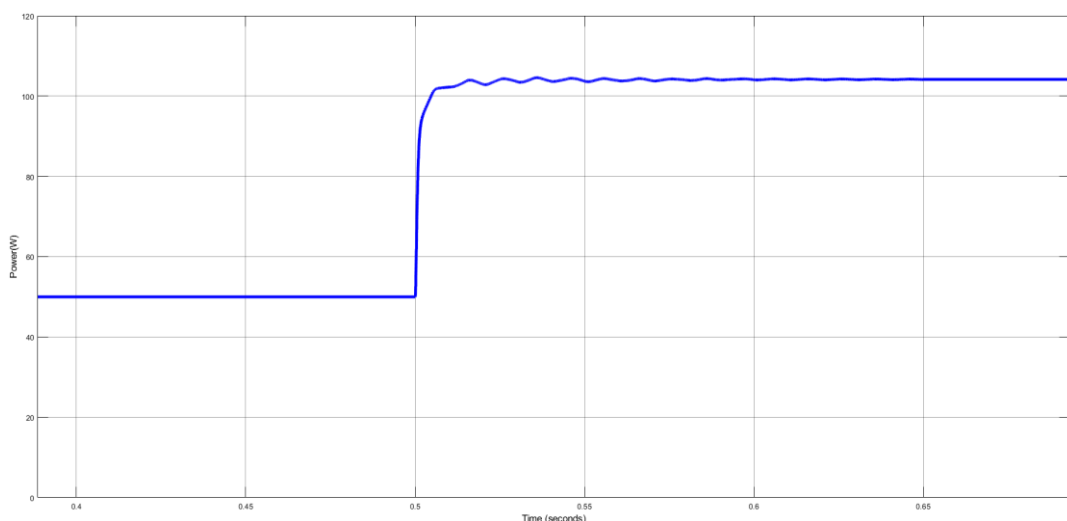


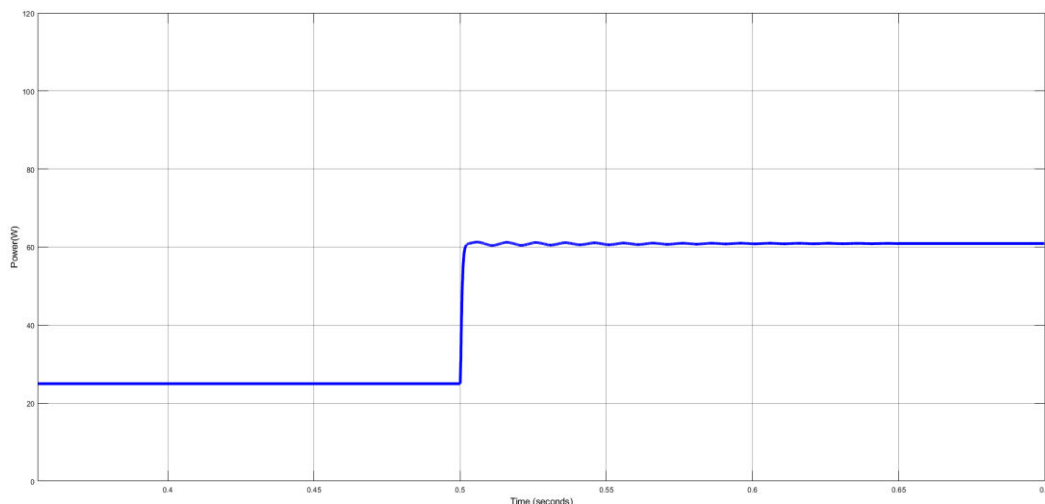
Fig 13: Voltage droop characteristics for load sharing and ANFIS control system (as simulated in MATLAB Simulink)

This plot displays the output power behaviour of Converter-1. Initially, the power level is steady at 50W. At approximately 0.5 seconds, a sudden step change in the system causes the converter to increase its power output. The power rises rapidly to around 100W, showing some small oscillations during the transition phase. These oscillations gradually settle, and the power output stabilizes at the new level. This indicates that Converter-1 effectively responds to the increased load demand, supplying double its original power after the disturbance.



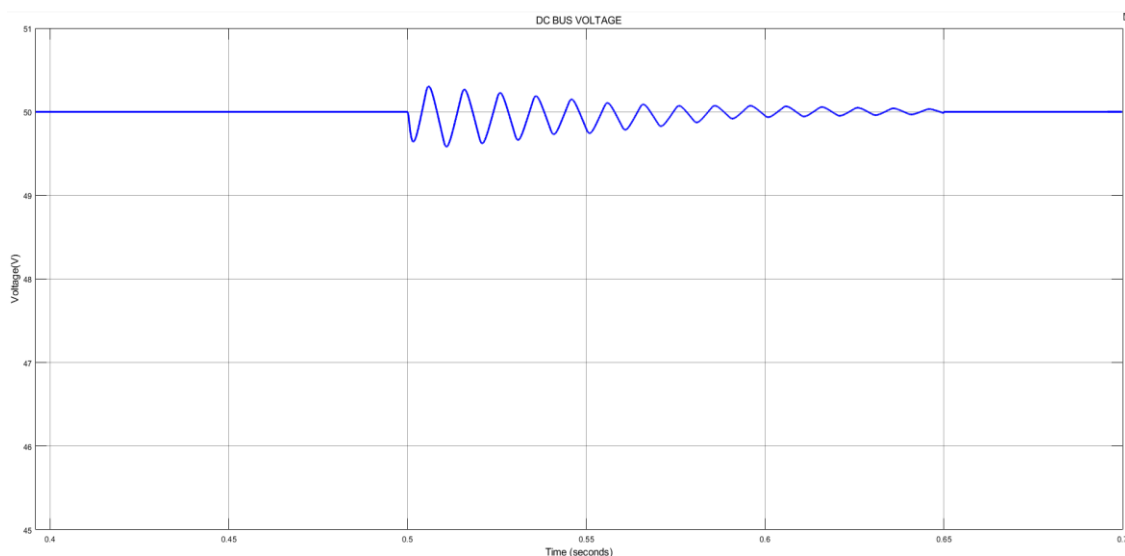
(a) Power of converter-1

In this graph, the power output of Converter-2 is shown. It starts at 25W before the step change occurs. Similar to Converter-1, there's a sudden rise in output around 0.5 seconds, where the power level jumps to approximately 50W. A few oscillations appear as the converter adapts, but it quickly reaches a steady state. This behaviour confirms that Converter-2 adjusts accordingly to maintain its role in the system, still supplying half the power of Converter-1 and maintaining the desired 1:2 power-sharing ratio.



(b) Power of converter-2

This graph shows how the DC bus voltage, set to a reference of 50V, responds to a sudden load change when the system is governed by an ANFIS (Adaptive Neuro-Fuzzy Inference System) controller. At around 0.5 seconds, a disturbance occurs, triggering a series of damped voltage oscillations. Despite the initial fluctuations, the ANFIS controller effectively handles the transient response. The oscillations gradually reduce in amplitude, and the voltage settles back to the set point of 50V. This illustrates the controller's capability to adapt to rapid changes and maintain voltage stability.



(c) DC bus Voltage

Fig 14: Load Sharing between two converters and DC bus voltage with proposed control activated.

CONCLUSION

Effective load sharing among several DC sources in a DC micro grid is achieved by an innovative control method that is introduced in this research. The suggested method guarantees efficient load sharing and system stability by integrating droop characteristics into DC-DC converters. To maintain a constant DC bus voltage under changing loading circumstances, the system is able to regulate the voltage-axis intercept of the droop characteristics. In addition, the ANFIS controller approach may improve the control system's transient responsiveness, leading to better performance.

REFERENCES

- [1] Pushkar Chaudhari, Mayuresh Khadse, Vinaya Jadhav, Parch Patel, Kaustubh Adware, Mute Raj wade, Hobbit Sharma College of Engineering, Pune "Novel Control Strategy for Dynamic Load Sharing Between DC-DC Converters for DC Microgrid".
- [2] Application Report,"AN-1197 Selecting Inductors for Buck Converters", April 2013, [online], Available: <http://www.ti.com/lit/an/snva038b/snva038b.pdf> [Accessed: June, 2014].
- [3] Dr. Varodom Toochinda," Digital PID Controllers", June 2011, [online], Available: <http://www.scilab.ninja/doc/b4/pid.pdf> [Accessed: Aug. 2014]
- [4] H. Kakigano, Y. Miura, and T. Ise, "Configuration and control of a DC micro grid for residential houses", in Proceedings of Transmission & Distribution Conference & Exposition: Asia and Pacific, 2009, pp. 1-4.
- [5] H. Kakigano, Y. Miura, and T. Ise, "Fundamental characteristics of DC micro grid for residential houses with cogeneration system in each house", in Proceedings IEEE Power and Energy Society General Meeting, 2008, pp. 1-6.
- [6] H. Kakigano, Y. Miura, T. Ise, and R. Uchida, "DC micro grid for super high quality distribution – system configuration and control of distributed generations and energy storage devices", in Proceedings IEEE Power Electronics Specialists Conference, 2006, pp. 1-7.
- [7] Muhammad H. Rashid "Power Electronics, Devices and Applications", 3rd ed.: Prentice Hall.
- [8] Liu, J.; Han, X.; Wang, L.; Peng, Z.; Jing, W. Operation and control strategy of DC Microgrid. Power Syst. Technol. 2014, 38, 2356–2362.
- [9] Ni, Y.; Xu, J. Analysis of Quasi-sliding-mode switching control for DC-DC converters. Chin. J. Electr. Eng. (Proc. CSEE) 2008, 28, 1–6.
- [10] Arian Azizi, Mohsen Hamzeh, "Stability Analysis of a DC Microgrid With Constant Power Loads Using Small-Signal Equivalent Circuit", 2020 11th Power Electronics, Drive

- Systems, and Technologies Conference (PEDSTC), pp.1-6, 2020.
- [11] Chunjiang Zhang, Meng Jiao, Mengna Liang, Ming Liu, Zhizhong Kan, "Power Control of Distributed Energy Storage System in Bipolar DC Microgrid", 2019 22nd International Conference on Electrical Machines and Systems (ICEMS), pp.1-6, 2019.
- [12] Abd Alelah Derbas, Mohsen Hamzeh, "A New Power Sharing Method for Improving Power Management in DC Microgrid with Power Electronic Interfaced Distributed Generations", 2019 27th Iranian Conference on Electrical Engineering (ICEE), pp.624-629, 2019.
- [13] Sonia Moussa, Manel Jebali-Ben Ghorbal, Ilhem Slama-Belkhodja, "DC voltage level choice in residential remote area", 2018 9th International Renewable Energy Congress (IREC), pp.1-6, 2018.
- [14] Amirhossein Tavassoli, Babak Allahverdinejad, Nasim Rashidirad, Mohsen Hamzeh, "Performance analysis of series SPOs in a droop-controlled DC microgrid", 2017 Smart Grid Conference (SGC), pp.1-6, 2017
- [15] Kumar, T. P., Ganapathy, S., & Manikandan, M. (2024). Voltage stability using optimized control on IOT based ANFIS. *Przegląd Elektrotechniczny*, 100. DOI:10.15199/48.2024.02.53
- [16] Balakishan, P., Chidambaram, I. A., & Manikandan, M. (2023). An ANN Based MPPT for Power Monitoring in Smart Grid using Interleaved Boost Converter. *Tehnički vjesnik*, 30(2), 381-389. DOI:10.17559/TV-20220820194302.
- [17] Quawi, A., Shuaib, Y. M., & Manikandan, M. (2023). Power quality improvement using ann controller for hybrid power distribution systems. *small*, 16, 21. DOI:10.32604/IASC.2023.035001.
- [18] Sathish, C., Chidambaram, I., & Manikandan, M. (2023). Hybrid Renewable Energy System with High Gain Modified Z-Source Boost Converter for Grid-Tied Applications. *Problemele Energeticii Regionale*, 57(1), 39-54. DOI:https://doi.org/10.52254/18570070.2023.1-57.04
- [19] Reddy, S. G., Ganapathy, S., & Manikandan, M. (2022). Power quality improvement in distribution system based on dynamic voltage restorer using PI tuned fuzzy logic controller. *Электротехникаиэлектромеханика*, (1 (eng)), 44-50. doi:https://doi.org/10.20998/2074-272X.2022.1.06
- [20] Babu, V., Ahmed, K. S., Shuaib, Y. M., & Manikandan, M. (2021). Power quality enhancement using dynamic voltage restorer (DVR)-based predictive space vector transformation (PSVT) with proportional resonant (PR)-controller. *IEEE Access*, 9, 155380155392. DOI:10.1109/ACCESS.2021.3129096

- [21] Babu, V., Ahmed, K. S., Shuaib, Y. M., & Mani, M. (2021). A novel intrinsic space vector transformation based solar fed dynamic voltage restorer for power quality improvement in distribution system. *Journal of Ambient Intelligence and Humanized Computing*, 1-16
- [22] Manikandan, M., & Basha, A. M. (2016). ODFD: Optimized dual fuzzy flow controller based voltage sag compensation for SMES-based DVR in power quality applications. *Circuits and Systems*, 7(10), 2959.
- [23] Manikandan, M., & Basha, A. M. (2013). Power quality compensation using SMES coil with FLC. *International Journal of Advances in Engineering & Technology*, 6(4), 1855.
- [24] Ashwanth, S., Manikandan, M., & Basha, A. M. (2014). Superconducting Magnetic Energy Storage System based Improvement of Power Quality on Wind/PV Systems. *International Journal of Emerging Technology and Advanced Engineering*, 4(4), 676-682.
- [25] Quawi, A., Shuaib, Y. M., & Manikandan, M. (2024). CNN based fault event classification and power quality enhancement in hybrid power system. *International Journal of Power Electronics and Drive Systems (IJPEDS)*, 15(3), 1851-1870.
<https://doi.org/10.11591/IJPEDS.V15.I3.PP1851-1870>